NACA

RESEARCH MEMORANDUM

LOW-SPEED STABILITY CHARACTERISTICS OF A COMPLETE MODEL WITH A WING OF W PLAN FORM

By Edward C. Polhamus and Robert E. Becht

Langley Aeronautical Laboratory
Langley Field, Va.

NATIONAL ADVISORY COMMITTEE
FOR AERONAUTICS

WASHINGTON

April 23, 1952

NATIONAL ADVISORY COMMITTEE FOR AERONAUTICS

RESEARCH MEMORANDUM

LOW-SPEED STABILITY CHARACTERISTICS OF A COMPLETE MODEL WITH A WING OF W PLAN FORM

By Edward C. Polhamus and Robert E. Becht

SUMMARY

An investigation was made of the low-speed static stability characteristics of a complete model equipped with a W wing. The lift-curve slope of the wing-fuselage combination was found to be in good agreement with that predicted by available wing-alone theory. In addition, the maximum lift coefficient for the wing-fuselage compared favorably with that obtained on a 45° conventional sweptback wing. Both the wing-fuselage combination and the complete model were longitudinally stable up through the stall. The complete model, however, showed some reduction in stability over the lift-coefficient range from 0.40 to 0.86. The drag due to lift increased rapidly as the lift coefficient was increased beyond 0.4, apparently because of flow separation at the wing-panel junctures. Some improvement in this behavior was obtained by a forward extension of the wing chord in the vicinity of the junctures.

The effective dihedral variation with lift coefficient was similar to the results obtained on sweptforward wings. The complete model was directionally stable through the maximum lift coefficient although, at a lift coefficient slightly below the maximum, the directional stability was only about one-fourth that at zero lift.

INTRODUCTION

Previous investigations have shown that highly sweptback wings of moderate to high aspect ratio may be characterized by longitudinal instability at high lift coefficients due to the severe tip separation associated with the spanwise boundary-layer flow of these wings. It was therefore proposed that wings having combined sweptback and sweptforward panels - that is, composite plan forms - be investigated since, for a given sweep angle, they would tend to minimize the boundary-layer build-up at the tip. The results of a previous investigation showed

that improvements in the pitching-moment characteristics at high-lift coefficients could be obtained with a composite-plan-form wing. (See reference 1.) Because there were indications that the additional wing junctures of this type of wing plan form might be detrimental to the drag characteristics at high speed, no further development was undertaken. Recently, much interest in composite wings has been stimulated because of structural advantage with respect to twist under load. Because of this renewed interest, it was considered desirable to investigate the low-speed stability characteristics of a complete model with a W plan-form wing. Included in this investigation are the results of some exploratory tests made in an attempt to reduce the early separation at the midsemispan juncture of the wing panels.

SYMBOLS

The system of stability axes employed, together with an indication of the positive forces, moments, and angles is presented in figure 1. The symbols used in this paper are defined as follows:

C_L	lift coefficient (Lift/qS)
C_X	longitudinal-force coefficient (X/qS)
C_Y	lateral-force coefficient (Y/qS)
C_l	rolling-moment coefficient (L/qSb)
C_m	pitching-moment coefficient (M/qS$\bar{c}$)
C_n	yawing-moment coefficient (N/qSb)
X	longitudinal force along X-axis (Drag = -X), pounds
Y	lateral force along Y-axis, pounds
Z	force along Z-axis (Lift = -Z), pounds
L	rolling moment about X-axis, foot pounds
M	pitching moment about Y-axis, foot pounds
N	yawing moment about Z-axis, foot pounds
q	free-stream dynamic pressure, pounds per square foot $\left(\frac{\rho V^2}{2}\right)$

[redacted]

S	wing area, square feet
$\bar{c}$	wing mean aerodynamic chord, feet
c	local streamwise chord, feet
b	wing span, feet
V	free-stream velocity, feet per second
A	aspect ratio $\left(b^2/S\right)$
ρ	mass density of air, slugs per cubic foot
α	angle of attack of wing-chord plane, degrees
ψ	angle of yaw, degrees
ϵ	effective downwash angle at tail, degrees
Λ	angle of sweep of quarter-chord line, degrees
i_t	angle of incidence of stabilizer with respect to fuselage center line, degrees
$\bar{c}_t$	horizontal-tail mean aerodynamic chord, feet
l_t	tail length from $\bar{c}/4$ to $\bar{c}_t/4$, feet
S_t	horizontal-tail area, square feet

Subscripts:

ψ	denotes partial derivative of a coefficient with respect to yaw, for example, $C_{l_\psi} = \frac{\partial C_l}{\partial \psi}$

DESCRIPTION OF MODEL

A three-view drawing of the model used in this investigation is presented in figure 2 and the ordinates of the fuselage, which was of fineness ratio 10, are presented in table I.

The wing of the model was of W plan form and had 45° sweep referred to the quarter-chord line, a taper ratio of 0.60, aspect ratio 6, and

[redacted]

an NACA 65A009 airfoil section parallel to the plane of symmetry. The break in the sweep line occurred at the midsemispan station. The horizontal tail had 45° sweepback referred to the quarter-chord line, a taper ratio of 0.60, aspect ratio 4, and an NACA 65A006 airfoil section parallel to the plane of symmetry. Photographs of the model on the support strut are presented as figure 3, and the details of the juncture modifications are given in figure 4. The model was made of wood bonded to steel reinforcing members.

TESTS AND CORRECTIONS

The tests were conducted in the Langley 300 MPH 7- by 10-foot wind tunnel at a dynamic pressure of 73.12 pounds per square foot which, for average test conditions, corresponds to a Mach number of about 0.22 and a Reynolds number of 1,580,000 based on the mean aerodynamic chord of 1.02 feet.

Two types of tests were made to determine the lateral characteristics of the model. The parameters, C_{n_ψ}, C_{Y_ψ}, and C_{l_ψ} were determined from tests through the angle-of-attack range at yaw angles of $\pm 5^\circ$ The lateral characteristics also were determined from tests through a range of yaw angles at constant angles of attack.

The angle-of-attack, drag, and pitching-moment results have been corrected for jet-boundary effects, computed on the basis of unswept-wing theory by the method of reference 2. Independent calculations have shown that the effects of sweep on these corrections are negligible. All coefficients have been corrected for blocking by the model and its wake by the method of reference 3.

Corrections for the small tare forces and moments produced by the support strut have been applied to the data.

Vertical buoyancy on the support strut, tunnel air-flow misalinement and longitudinal pressure gradient have been accounted for in the computation of the test data.

RESULTS AND DISCUSSION

Presentation of Results

A table summarizing the figures which present the results of the investigation is given on the following page.

[redacted]

Longitudinal Characteristics

The effect of tail incidence on the aerodynamic characteristics of the model in pitch is presented in figure 5. An experimental tail-off lift-curve slope of 0.065 was obtained for the test model, which is in fair agreement with the theoretical value of 0.062, calculated for wing alone from reference 4. The experimental lift-curve slope of the composite wing-fuselage combination also agrees fairly well with the value of 0.060 presented in reference 5 for a conventional 45° sweptback wing of the same aspect ratio at approximately the same Reynolds number as that of the present tests. The maximum lift coefficient of 1.14 obtained for the composite wing-fuselage combination also compares favorably with the value of 1.10 for the conventional plan form. The wing of reference 5 was 6 percent thick and had the same aspect ratio and taper ratio as that of the composite-plan-form wing.

Although the tail-off pitching moments were essentially stable up through the stall, the variation of the pitching moments with angle of attack (fig. 6) is similar to that obtained from wings experiencing leading-edge separation. The results of unpublished pressure distribution measurements seem to indicate the presence of this type of flow pattern. (A discussion of the leading-edge separation phenomenon can be found in reference 6.) With the tail on, the reduction in stability between $\alpha = 6^\circ$ and $\alpha = 14^\circ$ $C_L = 0.40$ to $C_L = 0.86$ can be attributed jointly to the effect of leading-edge separation and the passage of the horizontal tail through the wing wake, the latter probably having the greater effect. For this model either raising or lowering the horizontal tail from the position used may improve the complete-model stability at these lift coefficients. The dashed pitching-moment curve shown in figure 5 represents the data obtained on the previously mentioned conventional sweptback wing. The gain in stability for the composite wing-fuselage combination, relative to the conventional sweptback wing, is readily apparent at the intermediate and high lift coefficients.

A fuselage-alone drag coefficient of 0.006 at $\alpha = 0^\circ$ was obtained experimentally, as compared to 0.005 calculated by the method of reference 7. Included in the theoretical drag calculations for the

[redacted]

fuselage alone is an experimental drag increment for the fuselage base pressure. The fuselage-alone drag coefficients are based on wing area.

From the data obtained on the fuselage alone and the fuselage-tail configurations, a horizontal-tail lift-curve slope of 0.011, based on the wing area, is indicated in the low-angle range. When this lift-curve slope is based on the tail area, a value of 0.054 is obtained, which is in good agreement with the theoretical results of reference 8. In the presence of the wing, however, the lift-curve slope of the horizontal tail in the low-angle range is only about 0.036 based on the horizontal-tail area. This reduction in horizontal-tail lift-curve slope is due to the wing-induced downwash angles and is equivalent to a value of $\partial\epsilon/\partial\alpha$ of 0.34 which, as is shown later, is in good agreement with theory.

Figure 7 presents the downwash angles throughout the angle-of-attack range as obtained from figure 6 by the following method. A curve of the pitching-moment contribution of the horizontal tail was determined from the difference in the data obtained on the fuselage-tail configuration and the data on the fuselage alone at the same angles of attack. The resulting curve was assumed to be free of the induced downwash effects of the wing. Similarly, a curve of the pitching-moment contribution of the horizontal tail with downwash effects included was determined from the difference in the data obtained on the complete model and on the wing-fuselage configuration. At a given angle of attack on the curve obtained with the wing on, therefore, the effective downwash was considered to be the angle-of-attack difference between the two curves at the same pitching-moment value.

The parameter $\partial\epsilon/\partial\alpha$ was also calculated from reference 9 by using both the theoretical span-load distribution determined from reference 4, and the experimental span-load distribution from unpublished data. The resulting values for $\partial\epsilon/\partial\alpha$ were 0.26 and 0.32, respectively. The experimental value of $\partial\epsilon/\partial\alpha$ and the value calculated from the experimental span-load distribution therefore are in good agreement.

Wing-Juncture Modifications

Flow surveys behind the wing indicated separation in the wing-panel junctures at a lift coefficient of approximately 0.4. This separation probably contributed to the rapid increase in drag due to lift above this lift coefficient. In an attempt to delay this separation to higher lift coefficients by controlling the boundary-layer build-up in the junctures, a few exploratory tests were made with full-chord and half-chord

fences located on either side of the juncture. In addition, small vortex generators also were tried in the same location as the fences. The details and locations of the fences and vortex generators are given in figure 4. The attempts to reduce the separation in the juncture by the above methods were unsuccessful. (See figs. 8 and 9.)

Chord extensions located as shown in figure 4 were then investigated. The vortex from the tips of the chord extension was believed to have a tendency to oppose the natural boundary-layer flow along the panels. In addition, the vortex generated in this manner would increase with the angle of attack of the model as would the cross flow on the wing panels. Figure 10 shows that the model with a chord extension of 30 percent chord over 30 percent of the wing span had lower drag due to lift and a higher lift-curve slope. In addition, the nonlinearities of the pitching-moment curve were greatly reduced. Inasmuch as the coefficients are based on the original wing area, some reduction in the effect of chord extensions would be obtained if the additional area of the chord extensions were taken into account.

Lateral and Directional Stability Characteristics

The aerodynamic characteristics in yaw at various angles of attack of the wing-fuselage combination and the complete model are presented in figures 11 and 12, respectively. The lateral-stability parameters are presented in figure 13 for the same configurations.

The effective-dihedral variation with lift coefficient for both model configurations follows the pattern generally expected for sweptforward wings, that is, C_{l_ψ}/C_L is negative at low and intermediate lift coefficients. Inasmuch as the sweptforward outer panel has a longer moment arm than the sweptback inboard panel, it would be expected that the W wing would have an effective dihedral approaching that of a sweptforward wing. A theoretical C_{l_ψ}/C_L of -0.0030 was obtained from reference 10 for a conventional sweptforward wing alone of similar geometric characteristics; whereas the value -0.0025 was obtained experimentally on the complete model having the composite wing plan form. The vertical tail contributed a significant positive increment of effective dihedral at zero lift but gradually reduced to zero near a lift coefficient of 0.8.

The complete model remained directionally stable through the maximum lift coefficient although, at a lift coefficient slightly below the maximum, the directional stability was only about one-fourth that at zero lift. Good agreement was obtained in the vertical-tail contribution to the directional stability with that presented in reference 11 for a similar fuselage and tail configuration.

[redacted]

CONCLUSIONS

Low-speed wind-tunnel tests of a complete model equipped with a W type of wing indicated the following conclusions:

1. The lift-curve slope of the wing-fuselage combination was found to be in good agreement with that predicted by available wing-alone theory. In addition, the maximum lift coefficient for the wing-fuselage combination compared favorably with that obtained on a 45° conventional sweptback wing.

2. Both the wing-fuselage and the complete model were longitudinally stable through the stall; however, some reduction in stability occurred over the lift-coefficient range from 0.40 to 0.86.

3. The drag due to lift increased rapidly as the lift coefficient was increased beyond 0.4, apparently because of flow separation at the wing-panel junctures. Some improvement in this behavior was obtained by a forward extension of the wing chord in the vicinity of the junctures.

4. The effective dihedral variation with lift coefficient was similar to the results obtained on sweptforward wings. The addition of the tail to the model resulted in a significant positive increment in effective dihedral at zero lift that gradually reduced to zero near a lift coefficient of 0.8.

5. The complete model was directionally stable through the maximum lift coefficient although, at a lift coefficient slightly below the maximum, the directional stability was only about one-fourth that at zero lift.

Langley Aeronautical Laboratory
National Advisory Committee for Aeronautics
Langley Field, Va.

[redacted]

REFERENCES

1. Purser, Paul E., and Spearman, M. Leroy: Wind-Tunnel Tests at Low Speed of Swept and Yawed Wings Having Various Plan Forms. NACA TN 2445, 1951. (Supersedes NACA RM L7D23.)

2. Gillis, Clarence L., Polhamus, Edward C., and Gray, Joseph L., Jr.: Charts for Determining Jet-Boundary Corrections for Complete Models in 7- by 10-Foot Closed Rectangular Wind Tunnels. NACA ARR L5G31, 1945.

3. Herriot, John G.: Blockage Corrections for Three-Dimensional-Flow Closed-Throat Wind Tunnels, with Consideration of the Effect of Compressibility. NACA Rep. 995, 1950. (Supersedes NACA RM A7B28.)

4. Campbell, George S.: A Finite-Step Method for the Calculation of Span Loadings of Unusual Plan Forms. NACA RM L50L13, 1951.

5. Cahill, Jones F., and Gottlieb, Stanley M.: Low-Speed Aerodynamic Characteristics of a Series of Swept Wings Having NACA 65A006 Airfoil Sections. NACA RM L50F16, 1950.

6. Lange, Roy H., Whittle, Edward F., Jr., and Fink, Marvin P.: Investigation at Large Scale of the Pressure Distribution and Flow Phenomena over a Wing with the Leading Edge Sweptback 47.5° Having Circular-Arc Airfoil Sections and Equipped with Drooped-Nose and Plain Flaps. NACA RM L9G15, 1949.

7. Heaslet, Max A., and Nitzberg, Gerald E.: The Calculation of Drag for Airfoil Sections and Bodies of Revolution at Subcritical Speeds. NACA RM A7B06, 1947.

8. DeYoung, John, and Harper, Charles W.: Theoretical Symmetric Span Loading at Subsonic Speeds for Wings Having Arbitrary Plan Form. NACA Rep. 921, 1948.

9. Staff of Mathematics Division: Tables of Complete Downwash Due to a Rectangular Vortex. Rep. No. 10754 British A.R.C., July 21, 1947.

10. Toll, Thomas A., and Queijo, M. J.: Approximate Relations and Charts for Low-Speed Stability Derivatives of Swept Wings. NACA TN 1581, 1948.

11. Queijo, M. J., and Wolhart, Walter D.: Experimental Investigation of the Effect of Vertical-Tail Size and Length and of Fuselage Shape and Length on the Static Lateral Stability Characteristics of a Model with 45° Sweptback Wing and Tail Surfaces. NACA Rep. 1049, 1951. (Supersedes NACA TN 2168.)

[redacted]

TABLE I.- FUSELAGE ORDINATES

[Basic fineness ratio 12; actual fineness ratio 10 achieved by cutting off the rear one-sixth of the body.]

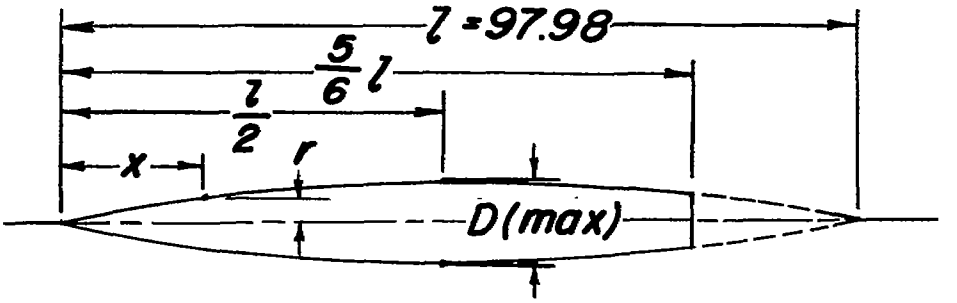

Ordinates			
x/l	r/l	x/l	r/l
0	0		
.005	.00231	0.4500	0.04143
.0075	.00298	.5000	.04167
.0125	.00428	.5500	.04130
.0250	.00722	.6000	.04024
.0500	.01205	.6500	.03842
.0750	.01613	.7000	.03562
.1000	.01971	.7500	.03128
.1500	.02593	.8000	.02526
.2000	.03090	.8333	.02083
.2500	.03465	.8500	.01852
.3000	.03741	.9000	.01125
.3500	.03933	.9500	.00439
.4000	.04063	1.0000	0.
L.E. radius: 0.00057l			

[redacted]

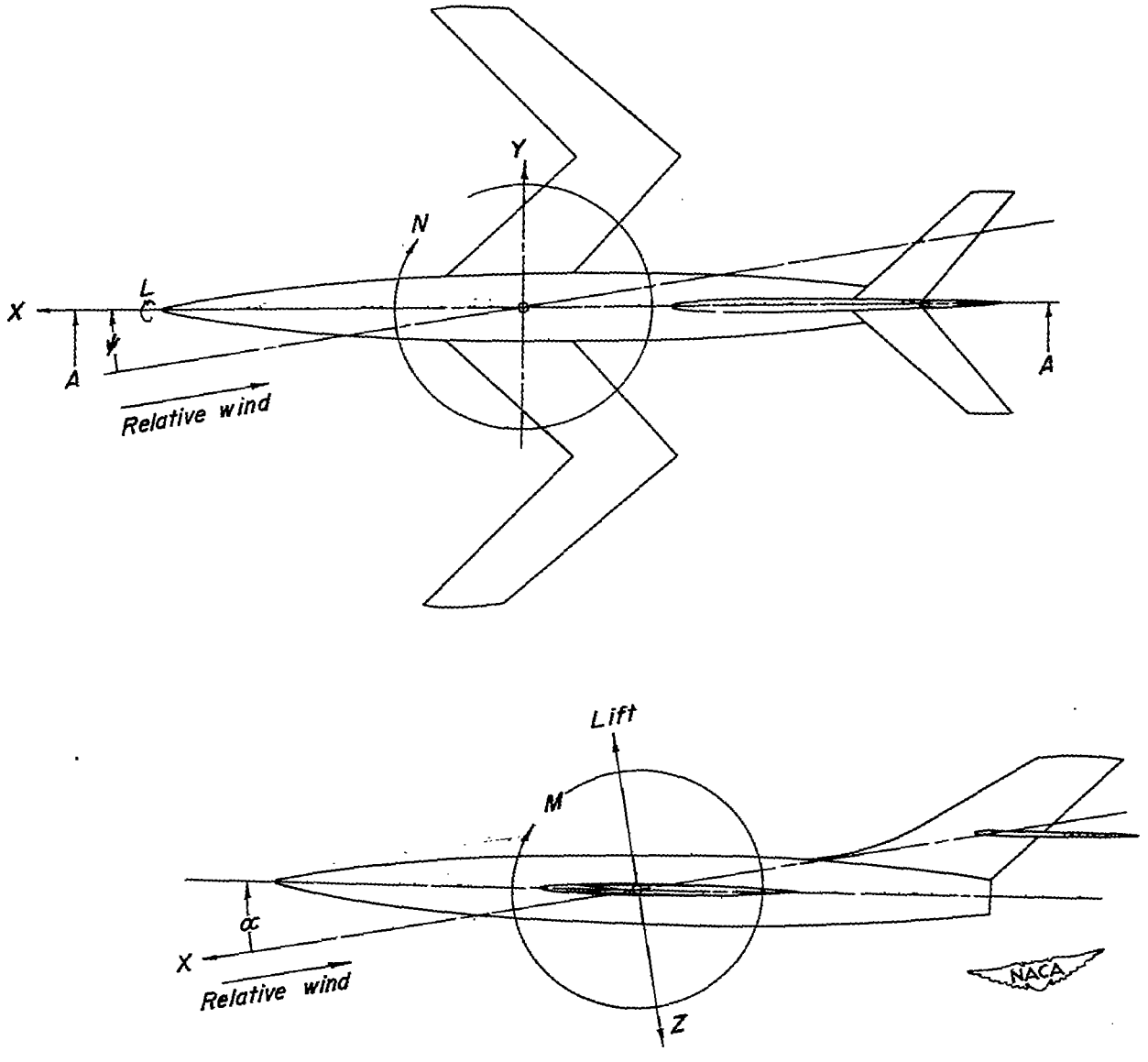

View A-A

Figure 1.- System of axes. Positive values of forces, moments and angles are indicated by arrows.

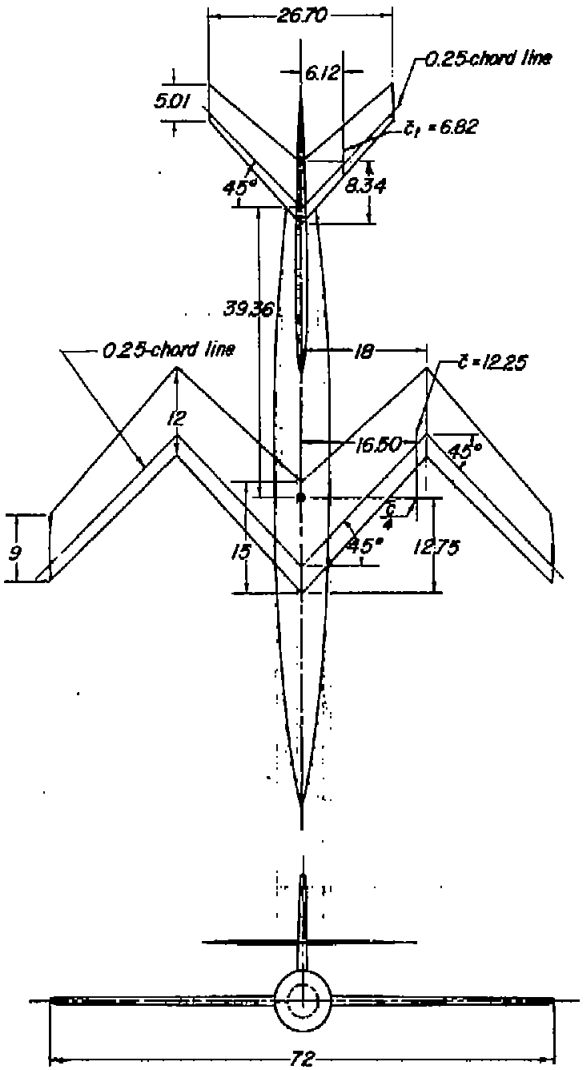

Physical characteristics

Wing	
Sweep of ¼, inboard panel, deg	*45*
Sweep of ¼, outboard panel, deg	*-45*
Area, sq ft	*6*
Span, ft	*6*
Aspect ratio	*6*
Taper ratio	*0.60*
Mean aerodynamic chord, ft	*1.02*
Incidence, deg	*0*
Dihedral, deg	*0*
Airfoil section parallel to free stream	*65A009*
Horizontal tail	
Area, sq ft	*1.24*
Aspect ratio	*4.00*
Airfoil section parallel to free stream	*65A006*
Vertical tail	
Area, sq ft	*1.69*
Aspect ratio	*1.18*
Airfoil section parallel to free stream	*63A009*

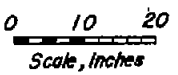

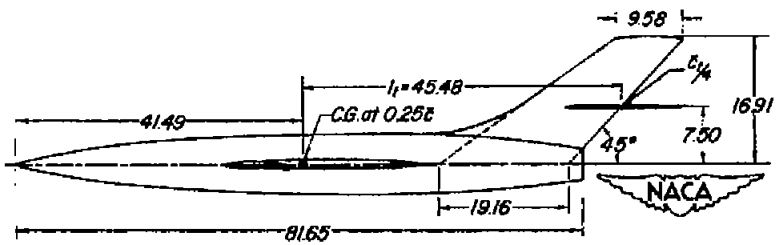

Figure 2.- General arrangement of test model.

Figure 3.- Photograph of model on support strut.

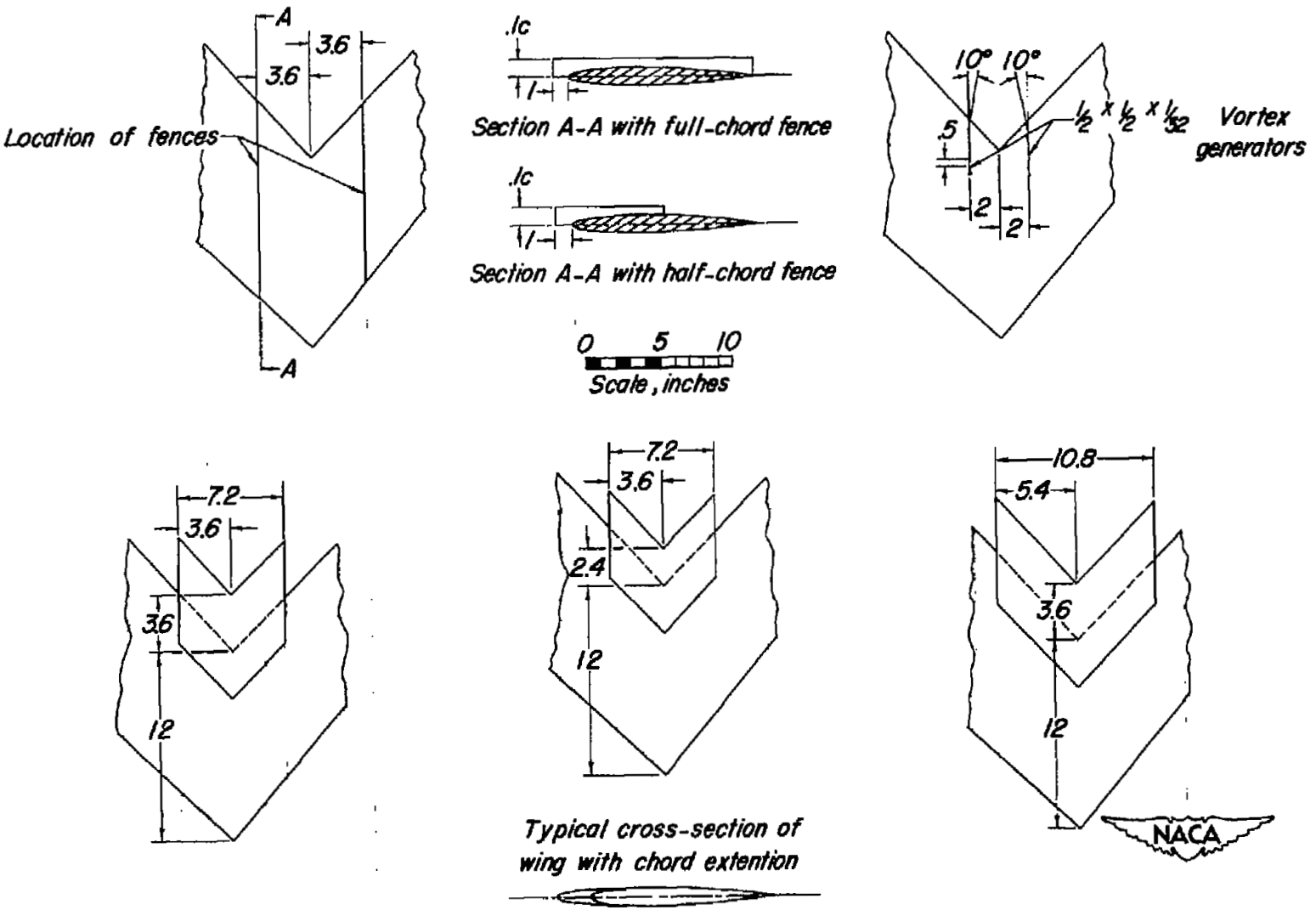

Figure 4.- Details of various wing-panel-juncture modifications.

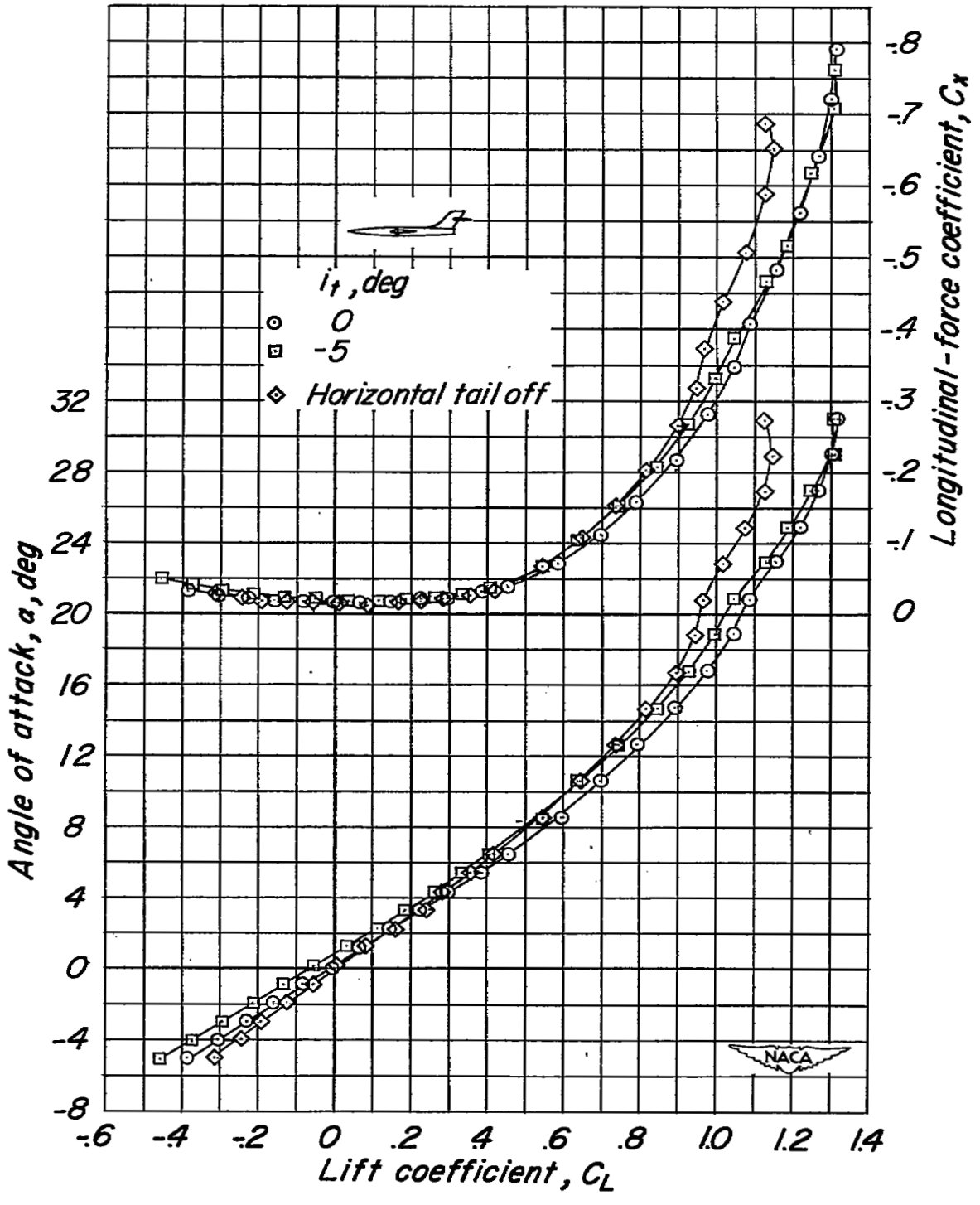

Figure 5.- Effect of tail incidence on the aerodynamic characteristics of the test model.

[redacted]

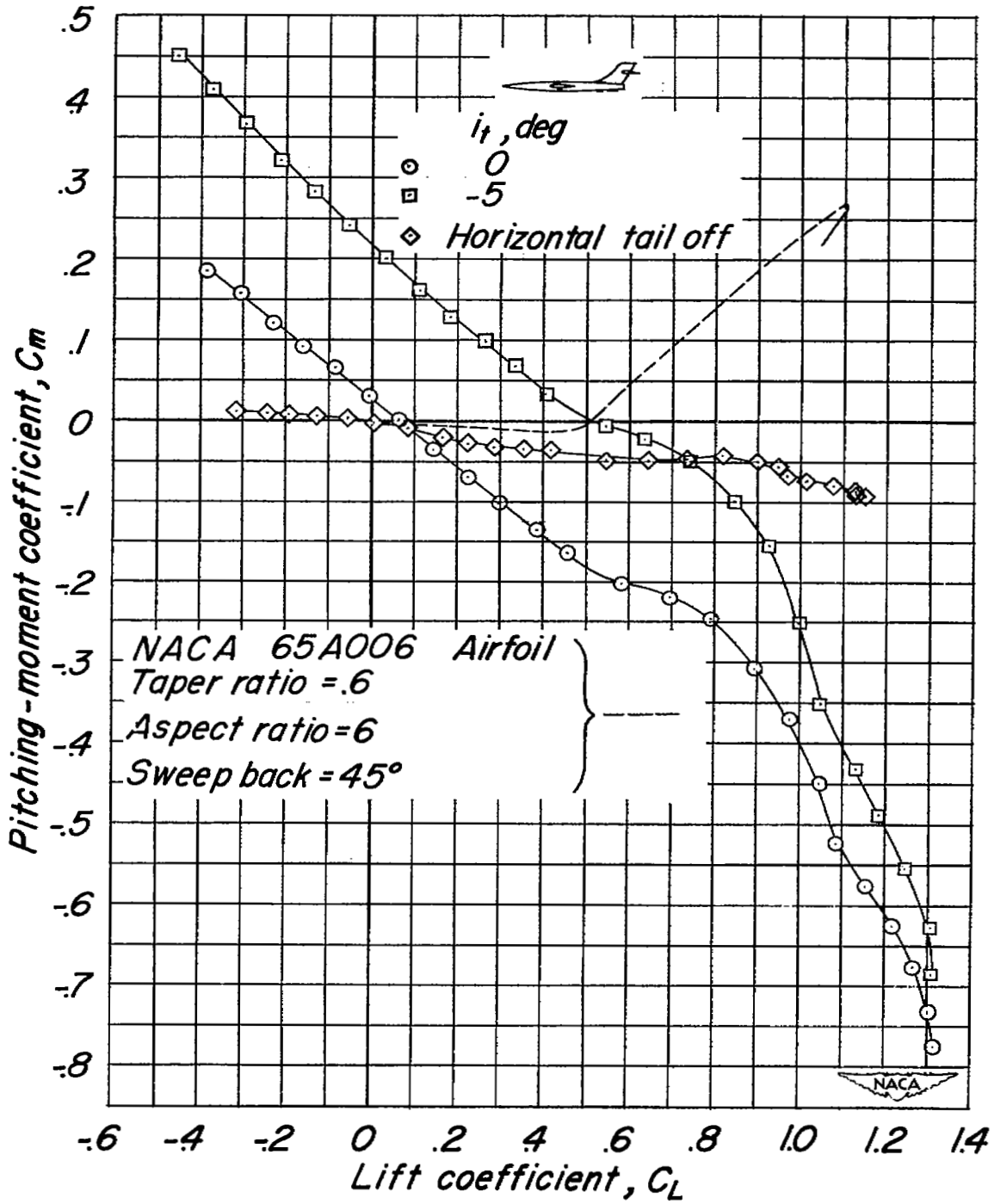

Figure 5.- Concluded.

[redacted]

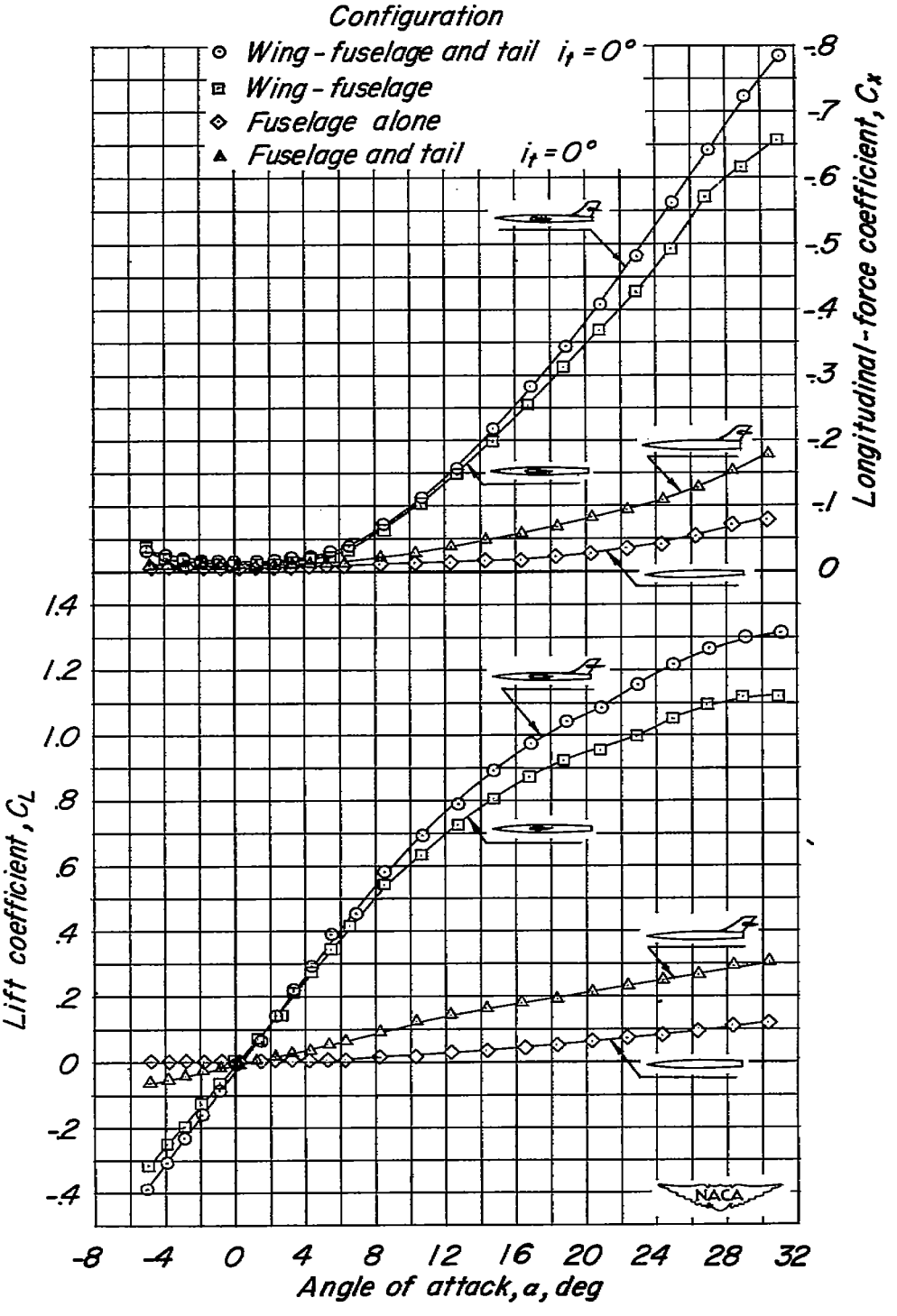

Figure 6.- Aerodynamic characteristics of the component parts of the test model.

[redacted]

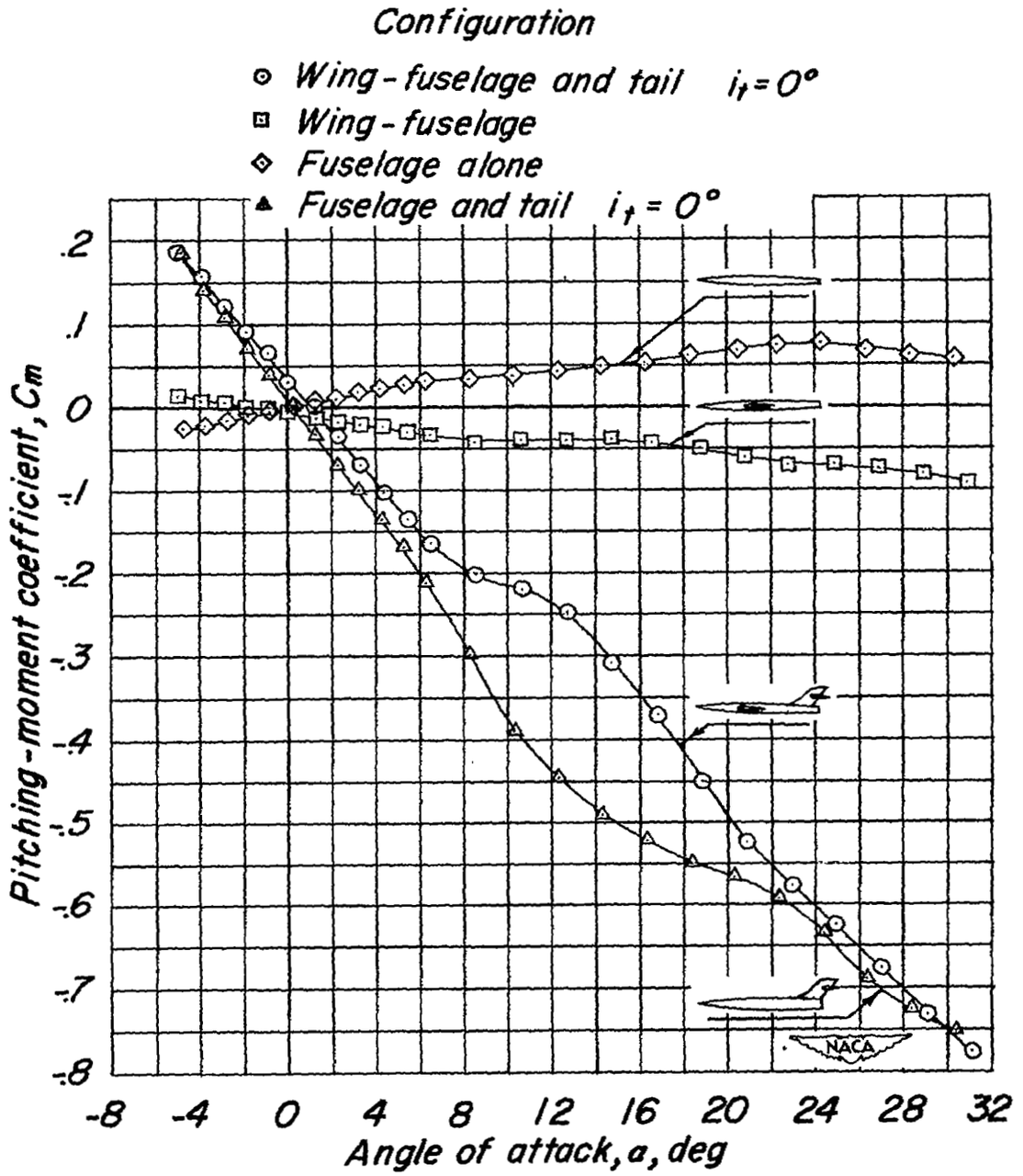

Figure 6.- Concluded.

[redacted]

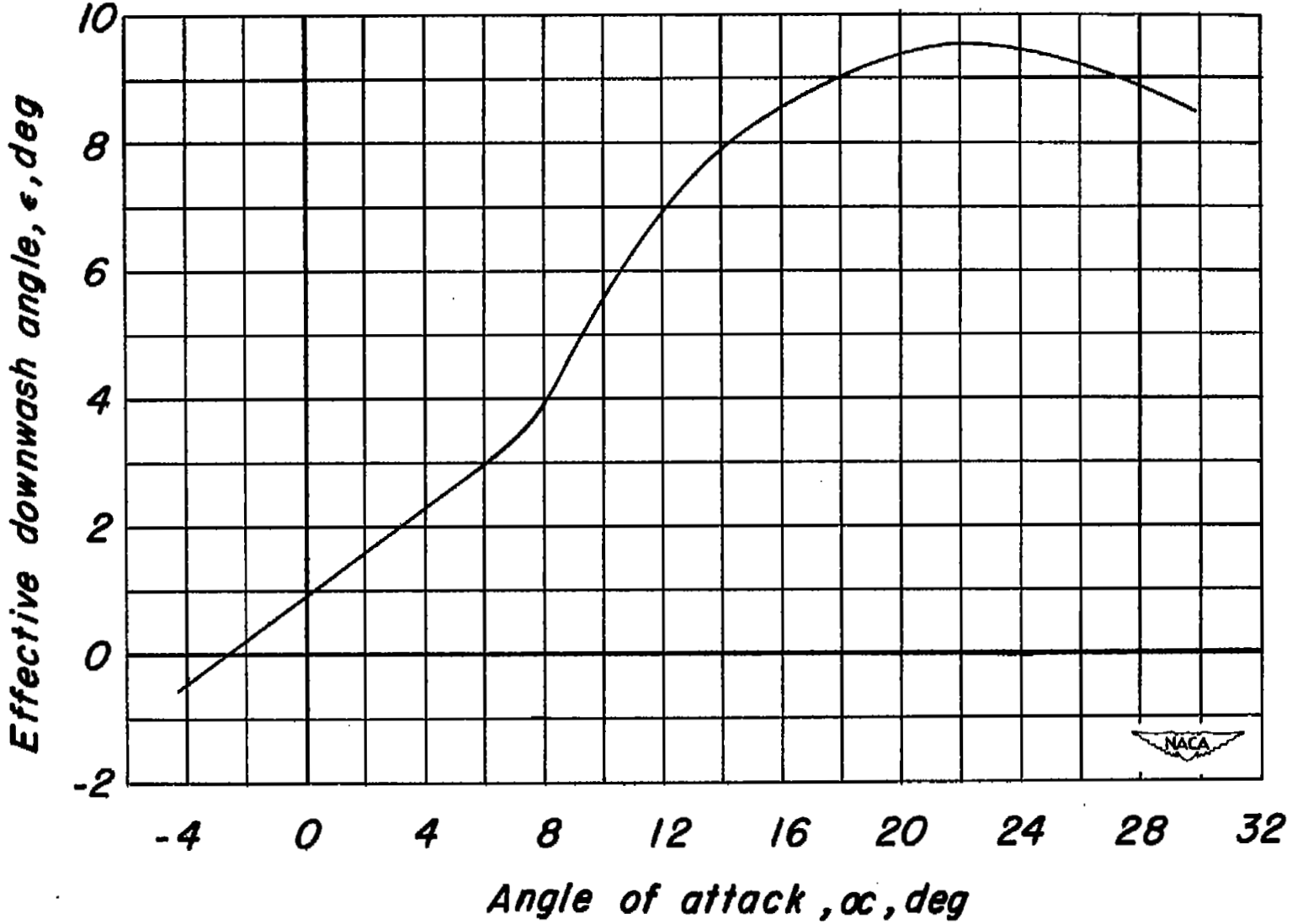

Figure 7.- Variation of effective downwash angle with angle of attack.

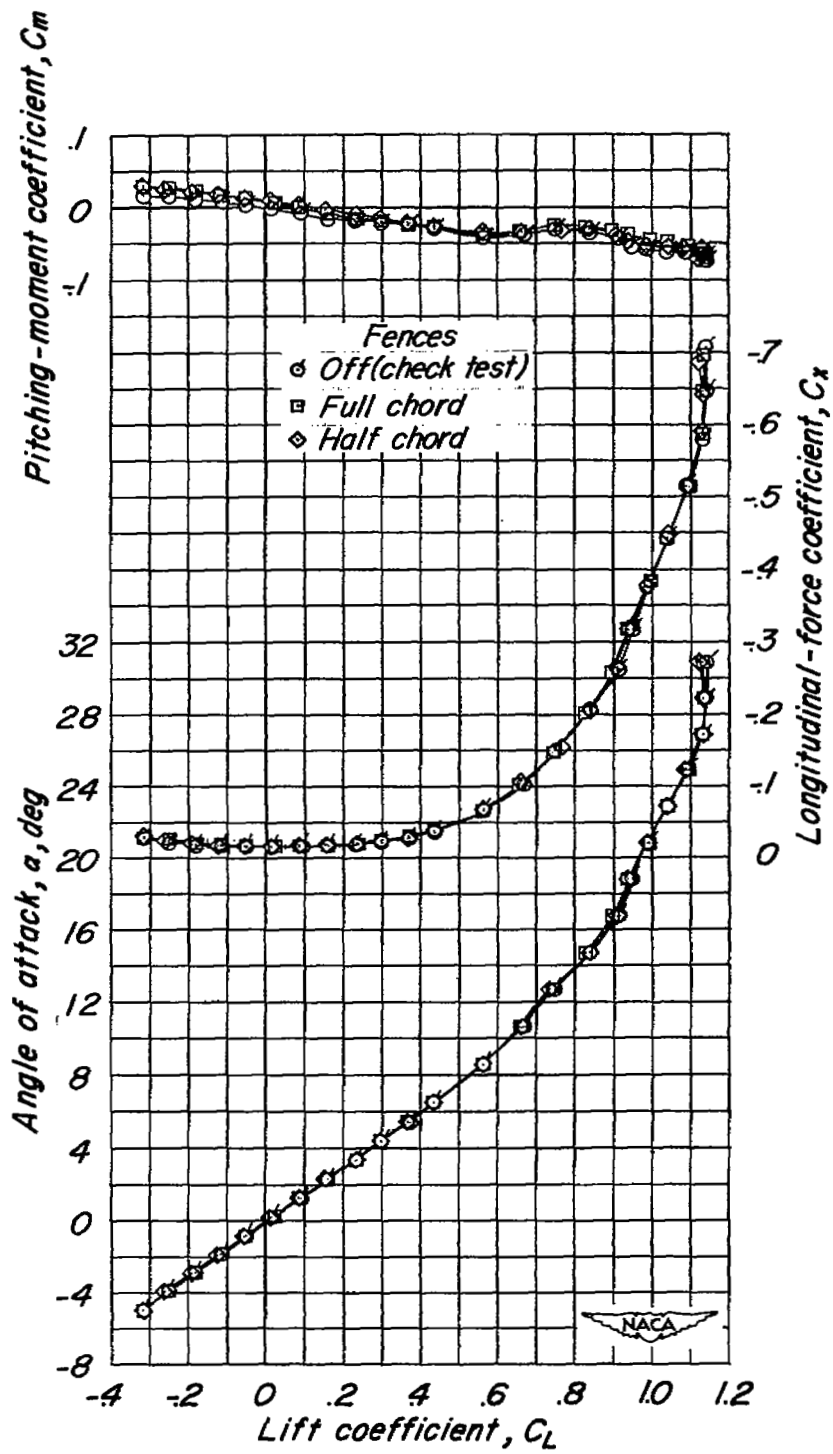

Figure 8.- The effect of wing fences on the aerodynamic characteristics of the test model. Horizontal tail off.

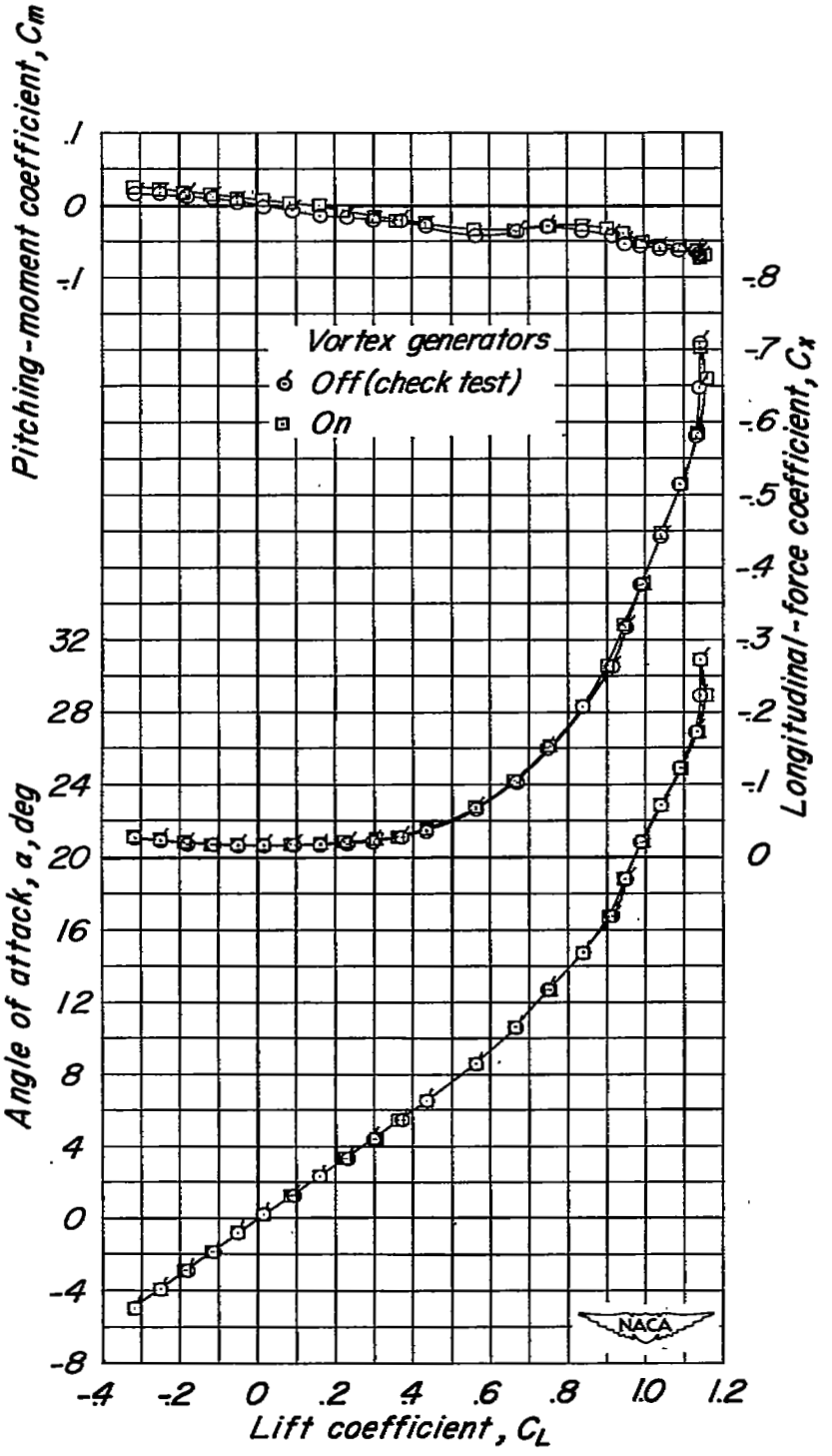

Figure 9.- The effect of vortex generators on the aerodynamic characteristics of the test model. Horizontal tail off.

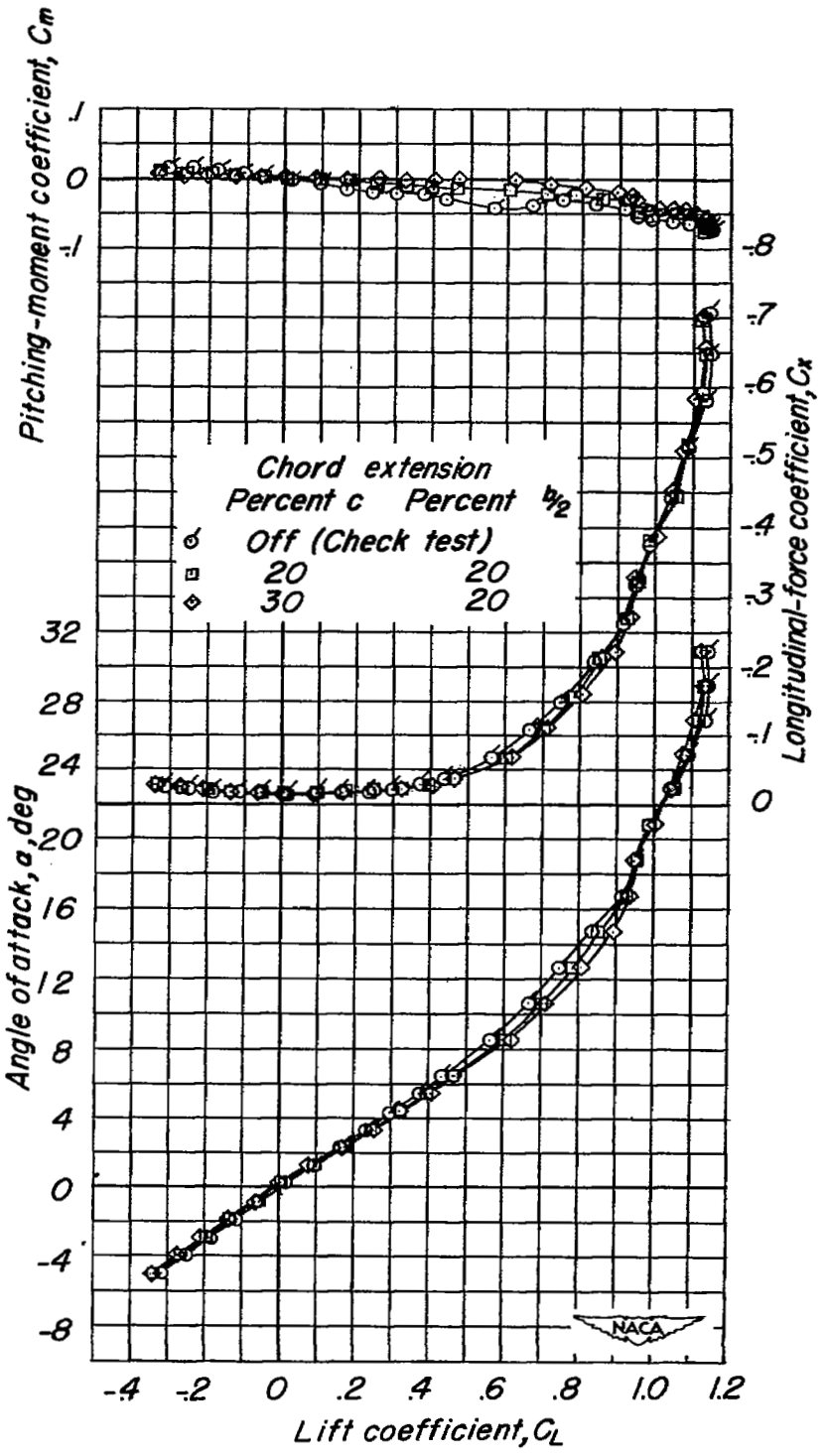

Figure 10.- The effect of chord extensions on the aerodynamic characteristics of the test model. Horizontal tail off.

[redacted]

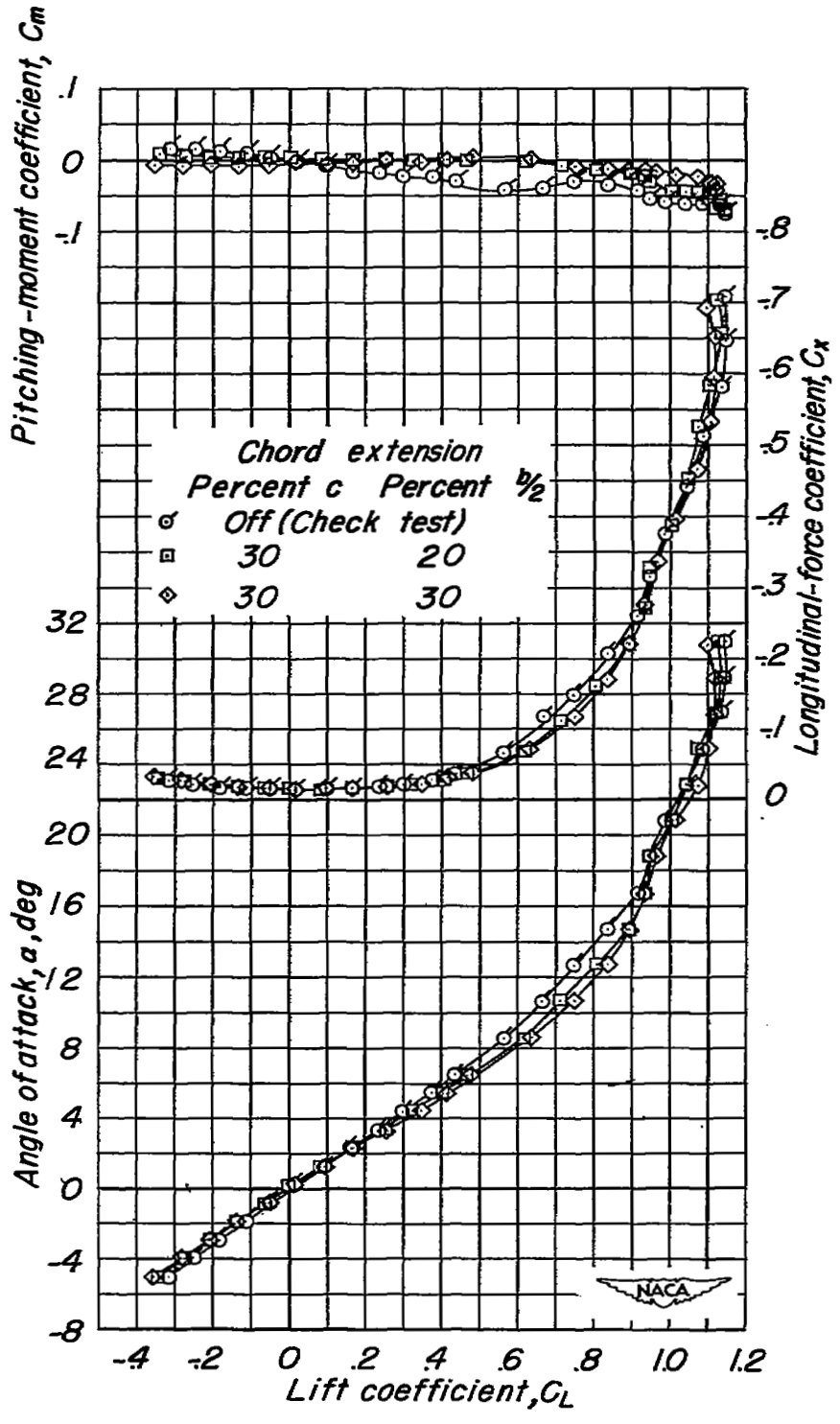

Figure 10.- Concluded.

[redacted]

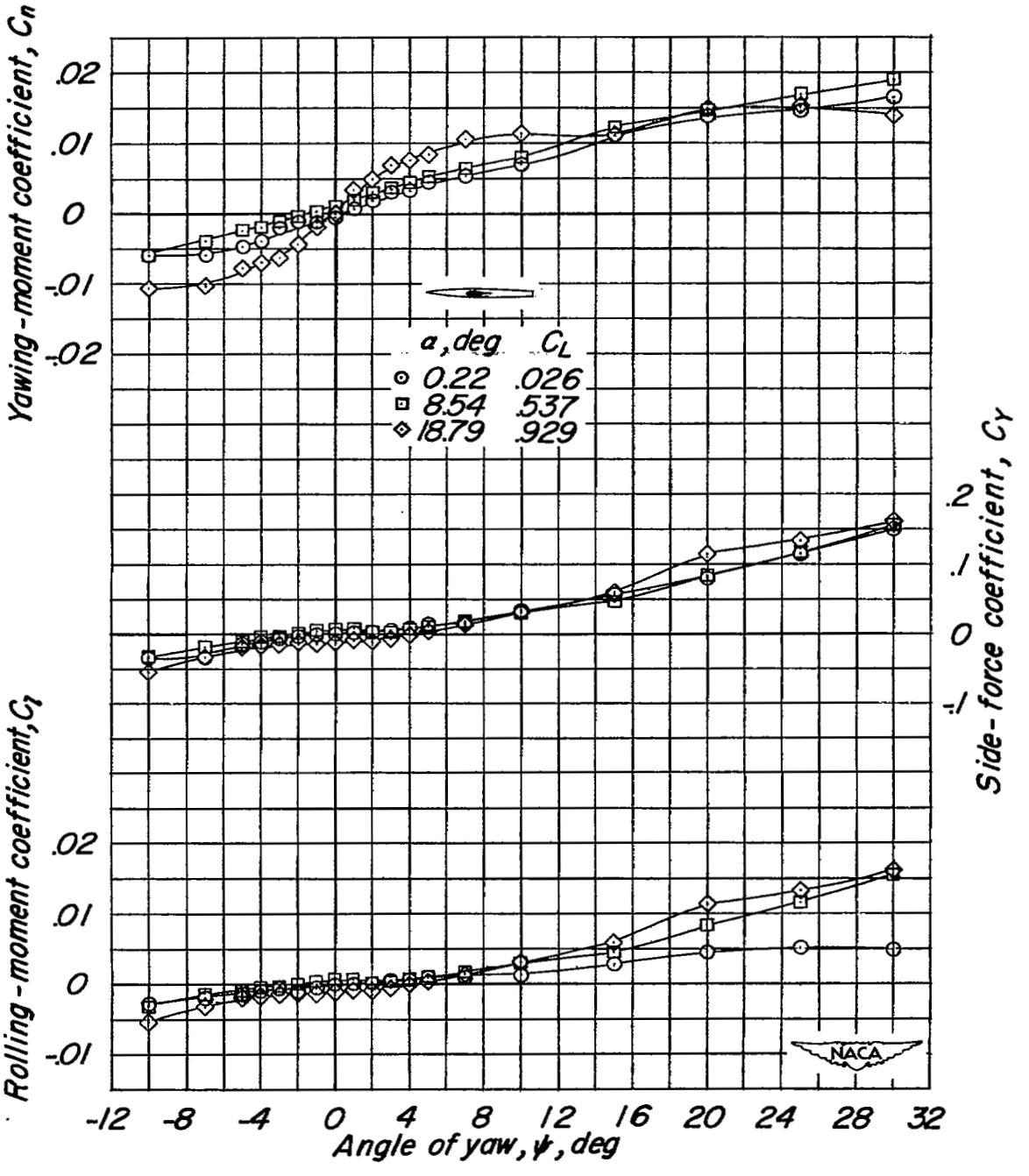

Figure 11.- The effect of angle of attack on the aerodynamic characteristics in yaw of the wing-fuselage combination.

[redacted]

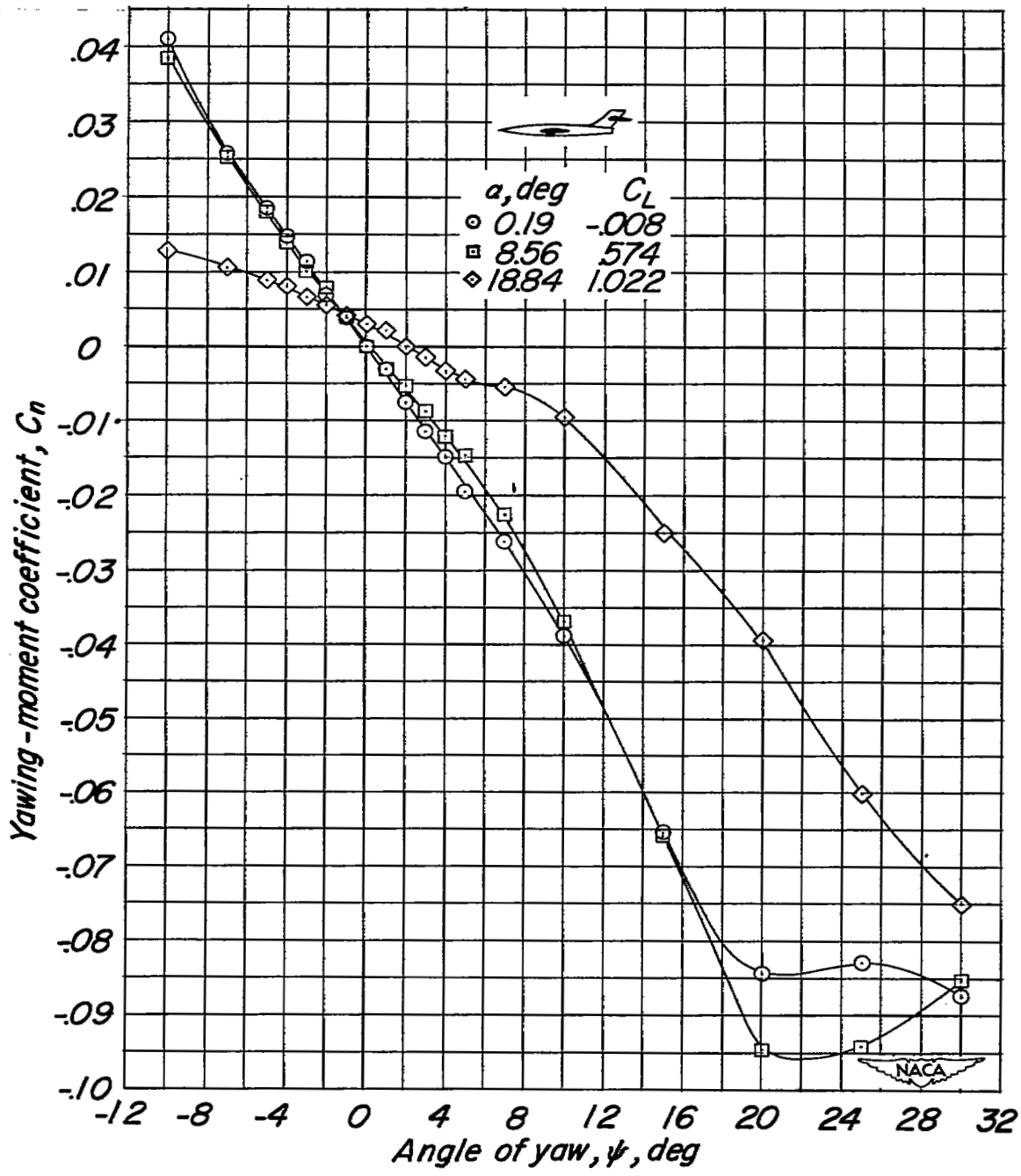

Figure 12.- The effect of angle of attack on the aerodynamic characteristics in yaw of the complete model. $i_t = 0^\circ$.

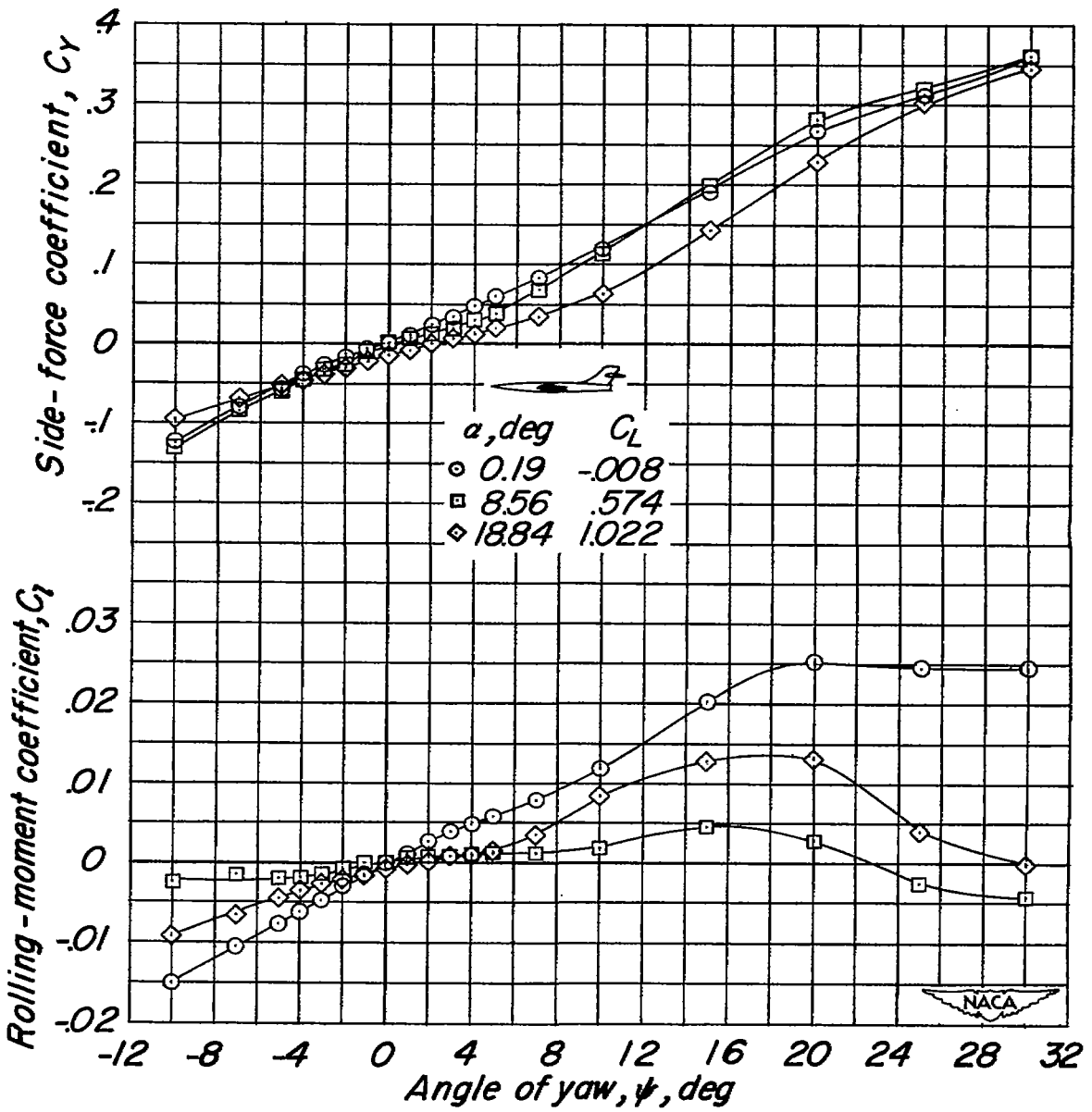

Figure 12.- Concluded.

[redacted]

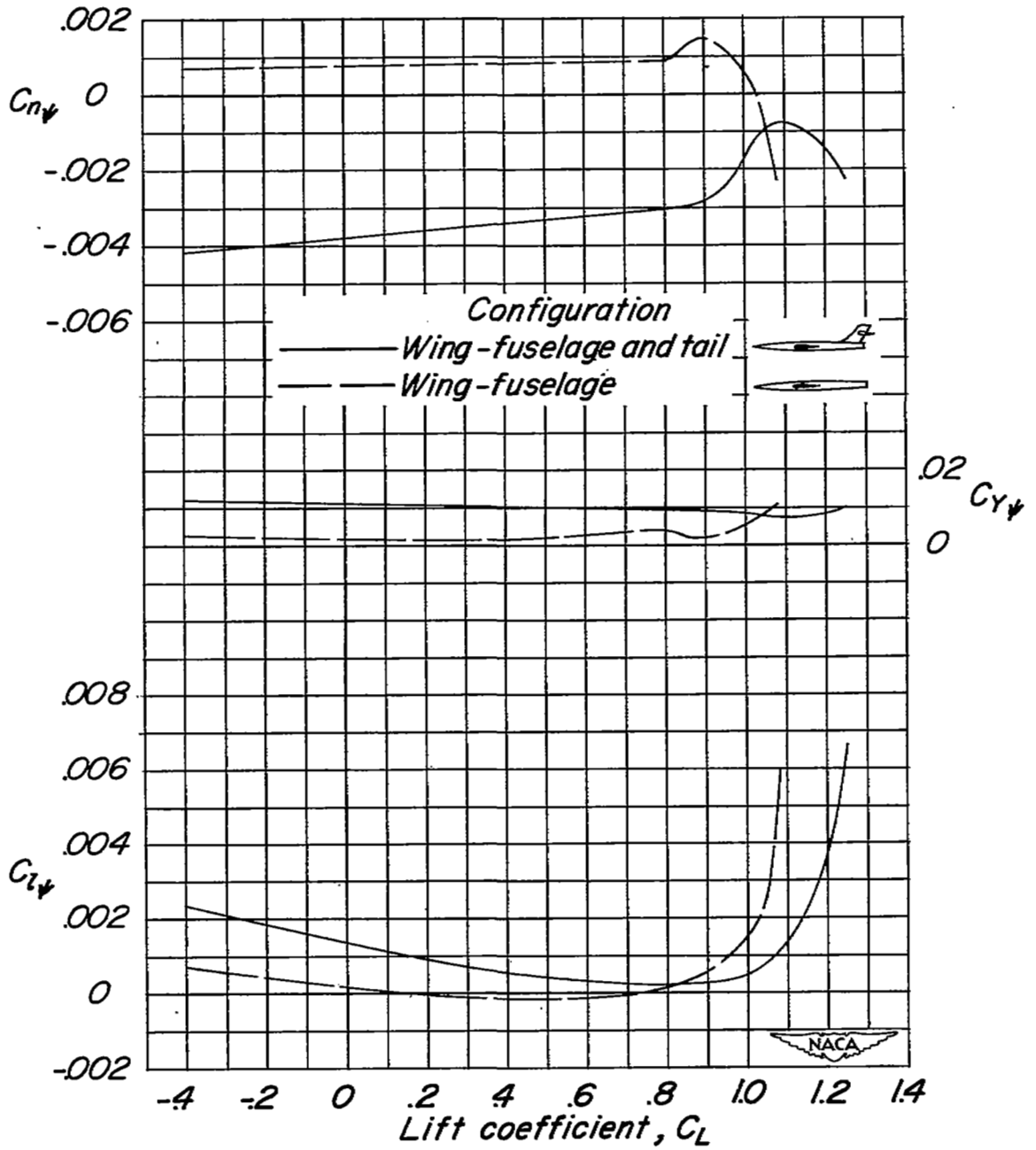

Figure 13.- The effect of the empennage on the lateral-stability parameters of the test model.